Giant Peroxisomes in Oleic Acid-induced *Saccharomyces cerevisiae* lacking the Peroxisomal Membrane Protein Pmp27p

Ralf Erdmann and Günter Blobel

Laboratory of Cell Biology, Howard Hughes Medical Institute, The Rockefeller University, New York 10021

Abstract. We have purified peroxisomal membranes from *Saccharomyces cerevisiae* after induction of peroxisomes in oleic acid–containing media. About 30 distinct proteins could be discerned among the HPLC- and SDS-PAGE–separated proteins of the high salt–extracted peroxisomal membranes. The most abundant of these, Pmp27p, was purified and the corresponding gene *PMP27* was cloned and sequenced. Its primary structure is 32% identical to PMP31 and PMP32 of the yeast *Candida biodinii* (Moreno, M., R. Lark, K. L. Campbell, and M. J. Goodman. 1994. *Yeast.* 10:1447–1457). Immunoelectron microscopic localization of Pmp27p showed labeling of the peroxisomal membrane, but also of matrix-less and matrix containing tubular membranes nearby. Electronmicro-

scopical data suggest that some of these tubular extensions might interconnect peroxisomes to form a peroxisomal reticulum. Cells with a disrupted *PMP27* gene (*Δpmp27*) still grew well on glucose or ethanol, but they failed to grow on oleate although peroxisomes were still induced by transfer to oleate-containing media. The induced peroxisomes of *Δpmp27* cells were fewer but considerably larger than those of wild-type cells, suggesting that Pmp27p may be involved in parceling of peroxisomes into regular quanta. *Δpmp27* cells cultured in oleate-containing media form multiple buds, of which virtually all are peroxisome deficient. The growth defect of *Δpmp27* cells on oleic acid appears to result from the inability to segregate the giant peroxisomes to daughter cells.

O NLY a few integral proteins of the peroxisomal membranes have been molecularly characterized in uni- and multicellular eukaryotes, using either genetic or reverse genetic methods. Pas3p from *Saccharomyces cerevisiae*, as well as PAF1 and PMP70 from mammalian cells, have been shown to be essential for peroxisome formation (Kamijo et al., 1990, 1992; Höhfeld et al., 1991, Tsukamoto et al., 1991; Shimozawa et al., 1992). A defect in the ALD protein causes X-linked adrenoleukodystrophy (Mosser et al., 1993). Functions for mammalian PMP22 (Kaldi et al., 1993) and PMP31, PMP32, and PMP47 from *Candida biodinii* (McCammon et al., 1990a: Moreno et al., 1994) have not yet been described. Hence, the peroxisomal membrane remains among the least characterized of the cellular membranes. A further challenge arises from the hypothesis by Lazarow et al. (1980) that peroxisomes of mammals are interconnected and form a peroxisomal reticulum. Lazarow proposed that this peroxisomal reticulum consists of at least two distinct domains: the classical bulbous peroxisomes and tubular extensions that interconnect the bulbous regions. Morphological evidence consistent with this pro-

posal has been presented (Gorgas, 1984; Lazarow and Fuyiki, 1985; Yamamoto and Fahimi, 1987; Lazarow, 1988; Baumgart et al., 1989; Leurs et al., 1993). At present, it is not known whether these morphologically distinct membrane domains are also biochemically and functionally distinct.

In yeasts grown under normal laboratory conditions, peroxisomes are among the least conspicuous organelles, consisting only of a few small and irregularly shaped entities with no evidence for a peroxisomal reticulum (Avers and Federman, 1968; Osumi et al., 1974; Veenhuis et al., 1979, 1987; Veenhuis and Goodman, 1990). Not surprisingly, these structures have resisted purification by conventional cell fractionation methods since their size and density are indistinguishable from other membrane-derived vesicles found in a postnuclear supernatant of a cell homogenate (Szabo and Avers, 1969). However, the situation changes dramatically after induction of peroxisome proliferation as a result of growing certain yeast species on certain carbon sources (Osumi et al., 1974; van Dijken et al., 1975; Roggenkamp et al., 1975; Fukui et al., 1975; Veenhuis and Harder, 1991). This peroxisome proliferation is characterized by an increase in the size and number of the organelles. The large size and dense matrix of induced peroxisomes (often containing paracrystalline bodies) has made it possible to separate them efficiently from other organelles of a postnuclear supernatant (Roggenkamp et al., 1975; Kamiryo et

al., 1982; Douma et al., 1985; McCammon et al., 1990b; Gould et al., 1992). This, in turn, has allowed molecular characterization of a few peroxisomal membrane proteins from *C. biodinii* by reverse genetic methods (McCammon et al., 1990a; Moreno et al., 1994).

In the yeast *S. cerevisiae*, proliferation of peroxisomes can be induced by growth in oleic acid–containing media (Veenhuis et al., 1987). Failure to grow on oleic acid has previously been used to characterize a number of genes, termed *PAS* (peroxisomal assembly) genes, whose products are involved in aspects of peroxisome biogenesis (Erdmann et al., 1991; Höhfeld et al., 1991; Wiebel and Kunau, 1992; van der Leij et al., 1993). Only one of these, Pas3p, is an integral membrane protein. While the function of Pas3p is still unknown, it remains the only integral peroxisomal membrane protein of *S. cerevisiae* that has been molecularly characterized. Moreover, although α-Pas3p antibodies decorate Pas3p on immunoblots, they failed to give detectable signals by immunofluorescence or immunoelectron microscopy (Höhfeld et al., 1991). Hence, an ultrastructural characterization of the membranes delimiting the peroxisomal compartment of *S. cerevisiae*, using antibodies as probes, has not yet been accomplished.

In this paper, we report the purification and characterization of peroxisomes from oleate-induced *S. cerevisiae*. The gene coding for one of the most abundant peroxisomal membrane proteins, Pmp27p (peroxisomal membrane protein of 27 kD), was cloned and sequenced. Immunolocalization of Pmp27p allowed us to detect membranes that extended from bulbous peroxisomes and that are likely to represent tubular peroxisomal appendices. Deletion of the *PMP27* gene yielded cells that grew normally on glucose or ethanol, but that were growth impaired on oleate. Unlike wild-type cells, where oleate induction typically yields 20–30 small peroxisomes, oleate-induced Δpmp27 cells showed only a few, but very large peroxisomes. Moreover, Δpmp27 grown on oleate showed multiple buds, most of which were peroxisome deficient. These data suggest that Pmp27p is essential for the maintenance of peroxisome morphology and inheritance in oleic acid–induced *S. cerevisiae*.

Materials and Methods

Strains, Growth Conditions, and General Methods

The yeast strains used in this study were *S. cerevisiae* wild-types UTL-7A (*MATa*, *ura3-52*, *trp1*/his3-11,15, leu2-3,112), SKQ2N (*MATa/α*, adel/+, +/ade2, +/his1) and W303 (*MATa/α*, ade2-1/ade2-1, ura3-1/ura3-1, his3-11,15/his3-11,15, trp1-1/trp1-1, leu2-3,112/leu2-3,112, can1-100/can1-100). Yeast complete (YPD) and minimal (SD) media have been described previously (Erdmann et al., 1989). Oleic acid medium (YNO) contained 0.1% oleic acid, 0.02% Tween 40, 0.1% yeast extract, and 0.67% yeast nitrogen base. For oleic acid induction, cells were precultured in SD containing 0.3% dextrose to midlog phase, shifted to YNO medium, and incubated for 9–12 h. When necessary, auxotrophic requirements were added according to Ausubel et al. (1992).

Whole cell yeast extracts were prepared from 30 mg of cells according to Yaffee and Schatz (1984).

Common recombinant DNA techniques, including enzymatic modification of DNA, Southern blotting, and double-stranded sequencing of plasmid DNA, were performed essentially as described by Ausubel et al. (1992). Yeast transformations were done according to Bruschi et al. (1987).

Isolation of Peroxisomes

Cells were collected by centrifugation (5 g wet wt/1.5 liter medium), washed twice with H_2O, and incubated for 10 min in 100 mM Tris/HCl, pH 9.4, 10 mM DTT at 30°C. Cells were washed with 1.2 M sorbitol, and cell wall digestion was performed with 0.75 ml 1.2 M sorbitol, 0.2 ml Glusulase (Du Pont Pharmaceuticals, Inc., Wilmington, DE), 2 ml 0.5 mg/ml Zymolyase 100T (ICN, Costa Mesa, CA) in 1.2 M sorbitol, 0.075 ml 10 mg/ml Mutanase (Novo Nordisk, Danbury, CT) in 1.2 M sorbitol/g of cells for 1–2 h at 30°C with occasional shaking. Spheroplasting was monitored microscopically. Cells were washed twice with 1.2 M sorbitol, loaded on a 10-ml cushion of 1.1 M sorbitol, 7.5% Ficoll 400, and centrifuged for 20 min at 5,000 g (HB4 rotor; Sorvall Instruments, Wilmington, DE). The cell pellet was resuspended in buffer A (5 mM MES, pH 6.0, 0.6 M sorbitol, 0.5 mM EDTA, 1 mM KCl, 1 mM PMSF, 1.25 μg/ml pepstatin, 1.25 μg/ml antipain, 1.25 μg/ml chymostatin, and 1.25 μg/ml leupeptin), and was homogenized at 4°C with a potter homogenizer (1,500 rpm). Unbroken cells were removed by 10 min centrifugation at 1,600 g (Sorvall H-1000B, 3,000 rpm). For high yield peroxisome preparations, SKQ2N homogenates from 60 g cells were sedimented for 30 min at 25,000 g (Sorvall HB4, 13,000 rpm) onto 5-ml cushions of 2 M sucrose in buffer B (5 mM MES, pH 6.0, 1 mM EDTA, 1 mM KCl, and 0.1% ethanol). Organelle pellets were resuspended in 40 ml buffer B and loaded onto eight continuous 24-ml 36–68% (wt/vol) sucrose gradients above cushions of 1.5 ml Purdenz (Accurate Chemical & Scientific Corp., Westbury, NY) and 1.5 ml 76.5% (wt/vol) sucrose. Centrifugation was performed for 2 h at 24,000 rpm (48,000 g) in a Sorvall TV850 rotor. Fractions (1.8 ml) were collected from the bottom, and aliquots prepared for SDS-PAGE. As judged by SDS-PAGE, immunoblotting, and catalase activity measurements, the peroxisomal peak fractions (fractions 4–6) were pooled and diluted fivefold by dropwise addition of 0.5 M sorbitol in buffer B. Organelles were sedimented onto a cushion of 2 M sucrose in buffer B at 27,000 g for 40 min (Sorvall HB4, 13,000 rpm). The organellar pellets were carefully resuspended in 20 ml 0.5 M sorbitol in buffer A, and they were loaded onto continuous 24 ml 20–40% (wt/vol) Accudenz gradients (formerly Nycodenz; Accurate Chemical & Scientific Corp.) containing an inverse 4.25–8.5% (wt/vol) sucrose gradient above cusions of 1.5 ml Purdenz and 1.5 ml 45% (wt/vol) Accudenz, 4.25% sucrose. Gradient centrifugation was performed as described above. 1.8-ml fractions were collected from the bottom, and aliquots were prepared for SDS-PAGE. As judged by SDS-PAGE and immunoblotting the peroxisomal peak fractions (fractions 5 and 6) were pooled, diluted fivefold with 0.5M sorbitol in buffer B, and centrifuged (Sorvall SA600, 13,500 rpm, 26,000 g, 40 min). Sedimented peroxisomes were processed for electron microscopy and membrane preparation.

For the subcellular localization of Pas3p at different timepoints of induction (see Fig. 2), UTL-7A homogenates (each 5 ml) were loaded onto continuous 25-ml 15–35% (wt/vol) Accudenz gradients with inverse 4.25–8.5% (wt/vol) sucrose gradients and cushions of 2 ml Purdenz and 2 ml 45% (wt/vol) Accudenz, 8.5% (wt/vol) sucrose. Gradients were in buffer B. Gradient centrifugation was performed as described above. The Purdenz was discarded, and 1.2-ml fractions were collected from the bottom. Taking the sucrose concentration into account, the density of the fractions was determined. 150 μl of each fraction was diluted in 1.35 ml 11.2% TCA, precipitated for 2 h on ice, and prepared for SDS-PAGE.

Successive Extraction of Peroxisomes

Peroxisome pellets (30 mg protein) were resuspended in 10 mM Tris/HCl pH 8.0, 1 mM PMSF, pooled, and incubated for 2 h on ice. The suspension was centrifuged for 10 min in a TLA 100.2 rotor (TL100; Beckman Instruments, Inc., Fullerton, CA) at 100,000 rpm (356,000 g_{av}). The supernatant was saved, the pellet was resuspended in 0.5 ml 10 mM Tris/HCl, pH 8.0, 1 mM PMSF, and incubated on ice for 1 h. The suspension was loaded on a 0.5 ml cushion of 10 mM Tris/HCl, pH 8.0, 1 mM PMSF, 250 mM sucrose and centrifuged as above. The supernatant was saved, the pellet was resuspended in 1 ml 10 mM Tris/HCl, pH 8.0, 0.5 M KCl incubated on ice for 30 min, and centrifuged as above. The supernatant was saved, the pellet was resuspended in 0.5 ml 10 mM Tris/HCl, pH 8.0, 0.5 M KCl, and incubated on ice for 30 min. 25 μl of the solution were sedimented for 60 min in a Beckman TLA-45 rotor at 109,000 g (45,000 rpm) and the membrane pellet was processed for electron microscopy. The remaining 475 μl were loaded on a cushion of 0.5 ml 10 mM Tris/HCl, pH 8.0, 250 mM sucrose, and centrifuged in the TLA 100.2 rotor as above. The resulting pellet was resuspended in 0.5 ml 0.1 M sodium carbonate (Fuyiki et al., 1982) and incubated for 30 min on ice, loaded on a 0.5-ml cushion of 0.1 M sodium carbonate, 250 mM sucrose, and centrifuged as above. All corresponding supernatants were pooled and, together with the final membrane pellet, processed for SDS-PAGE and immunoblotting.

Purification and Amino Acid Sequencing of Pmp27p

High salt-extracted peroxisomal membranes were prepared from oleic acid-induced SKQ2N cells. Further separation of the peroxisomal membrane proteins was achieved by reverse-phase HPLC. The peroxisomal membranes (~1 mg protein) were solubilized in 4% SDS, 10 mM Tris/HCl, pH 7.4, diluted fivefold in 200 mM Tris/HCl, pH 7.4, 20 mM DTT, and heated for 10 min at 60°C. Insoluble debris was removed by centrifugation in a microfuge for 10 min, and the soluble fraction was loaded onto a Aquapore butyl (C4) column (100 × 10 mm; Brownlee Labs, Applied Biosystems, Inc., Foster City, CA) equilibrated with 60% formic acid. After a 5-min linear increase to 9.9% acetonitrile in 60% formic acid, the column was eluted with a linear gradient of 32 ml 9.9%–33.0% acetonitrile in 60% formic acid, and 0.4-ml fractions were collected. Eluted fractions were dried in a Speed Vac concentrator (Savant Instruments Inc., Hicksville, NY), and pellets were solubilized in SDS sample buffer and analyzed by SDS-PAGE.

For sequencing of Pmp27p, the SDS samples of HPLC fractions containing this protein (fractions 52–57) were pooled and separated on a 12% polyacrylamide gel. Polypeptides were electrophoretically transferred on a polyvinyldiene difluoride membrane and visualized with 0.1% amidoblack in 10% acetic acid. Pmp27p was excised and subjected to NH_2-terminal sequence analysis on a gas phase sequenator (Applied Biosystems).

Isolation and Sequencing of PMP27

A *PMP27*-specific probe was generated by the PCR. According to the obtained NH_2-terminal sequence of Pmp27p, degenerate sense [5′ATGGAT-CCGA(CT)ACITT(AG)GT(AGCT)TA(CT)CA(CT)CC3′] and antisense [5′AAGAATTC(CT)AAIAC(CT)TT(CT)TC(CT)CT(AGCT)CC3′] oligonucleotide primers were synthesized, and the corresponding genomic region of the *PMP27* gene was amplified by the polymerase chain reaction with yeast genomic DNA (100 µg; Promega Corp., Madison, WI) as template. The amplification product of the expected size was isolated and subcloned into pBluescript KS(+) (Stratagene, La Jolla, CA), resulting in pKS27-1. The authenticity of the insert was confirmed by sequencing. The [^{32}P]dATP-labeled 90-bp insert was used to screen a genomic library (Rose et al., 1987), as well as a subgenomic library from *S. cerevisiae*. For the construction of the subgenomic library, *S. cerevisiae* genomic DNA was digested with EcoRI, and fragments of 3–4 kb were isolated and subcloned into pBluescript SK(+) (Stratagene), yielding ~50,000 independent clones. The screenings were performed in aequous solution according to Ausubel et al. (1992). Plasmid DNAs from positive clones were isolated, and the presence and location of *PMP27* were confirmed by restriction analysis and Southern blotting (Ausubel et al., 1992). Plasmid p27-1, containing a 3.8-kb EcoRI fragment, was isolated from the subgenomic library. A 2.2-kb ClaI/SpeI fragment of p27-1, which correspond to the entire *PMP27* gene plus 5′ and 3′ noncoding regions, was subcloned into pBluescript SK+, resulting in p27-10. DNA sequence analysis was performed by using the DNAstar software programs (DNAstar, Madison, WI). For complementation studies, the 2.2-kb insert of p27-10 was subcloned into the yeast *CEN*-plasmid pCS20 (Erdmann, 1994), resulting in pCSp27.

Epitope Tagging of Pmp27p

For immunolocalization studies on Pmp27p, an epitope tag encoding 10 amino acid residues from the influenza virus hemagglutinin antigen (HA)[1] (Wilson et al., 1984; Field et al., 1988) plus two flanking glycines as a spacer were inserted at the COOH terminus of the protein. For the insertion of the epitope tag into Pmp27p, a BglII site was introduced in front of the stopcodon of the *PMP27* gene by the polymerase chain reaction. In parallel, a BamHI site was introduced behind the stop codon to facilitate further subclonings. The two complementary oligonucleotides, yHA-1 and yHA-2 (Wozniak et al., 1994), with the following sequence

```
5′  gat ctt ggt tac cca tac gac gtc cca gat tac gct agc ggt 3′        yHA-1
      3′  aa cca atg ggt atg ctg cag ggt cta atg cga tcg cca g 5′        yHA-2
          G   Y   P   Y   D   V   P   D   Y   A   S   G    amino acid
                                                          residues
```

were annealed and inserted into the BglII site. Clones containing the se-

quence in the proper orientation were identified by DNA sequencing. For expression in yeast, the fragment encoding the tagged Pmp27p was subcloned in front of the *CYC1* terminator of the yeast *CEN* plasmid pCS20 (Erdmann, 1994), resulting in pCSp27TAG. Transformation of Δ*pmp27* mutant cells with either pCSp27 or pCSp27TAG resulted in a functional complementation of the mutant phenotype. The corresponding transformants were named Δ*pmp27* [Pmp27p] or [Pmp27p-HA], respectively.

Disruption of the PMP27 Gene

Disruption of the *PMP27* gene was performed by integrative transformation using the procedure of Rothstein (1991). In the construct used for the gene replacement, the 537-bp XbaI/PstI fragment of p27-10, encoding amino acids 19–198 of Pmp27p, was replaced by the *LEU2* containing 1.8 kb XbaI/PstI fragment of pJJ282 (Jones and Parkash, 1990). In the construct for integration, the *LEU2* gene was flanked by 710 bp of the 5′ side and by 973 bp of the 3′ side from the *PMP27* genomic locus. The linearized fragment was transformed into the *S. cerevisiae* diploid strain W303, and Leu$^+$ transformants were isolated. Heterozygous diploids carrying the integrated *pmp27::LEU2* disrupted gene and the wild-type *PMP27* were identified by Southern blotting. Blots were probed with the 90 bp ^{32}P-labeled PCR product described above under conditions described for the library screenings. Cells were sporulated, and tetrad analysis was performed. The expected 2:2 segregation for the Leu$^+$ marker was observed, and spores were tested for their ability to grow on oleic acid medium. One of the spores that contained the *pmp27::LEU2* disruption gene was designated Δ*pmp27*, and it was used for further studies.

Immunofluorescence Microscopy

Immunofluorescence microscopy was performed essentially according to Rout and Kilmartin (1990) with modifications described by Erdmann (1994). When the maintenance of cell buds was desired, cells were washed extensively and fixed with 3.7% formaldehyde for 10 min at 20°C before cell wall digestion. Rabbit antiserum against the yeast thiolase (Erdmann and Kunau, 1994; dilution = 1:3000), monoclonal 12CA5 antiserum against the HA-tag (BAbCO, Richmond, CA; dilution = 1:20), and 6-µg/ml solutions of Texas red–conjugated donkey anti-rabbit IgG (ICN) or FITC-conjugated donkey anti-mouse IgG (ICN) were used for the detection.

Electron Microscopy

For the morphology of peroxisomes and high salt-extracted peroxisomal membranes, pellets were fixed in 2.5% glutaraldehyde in 0.1 M cacodylate, postfixed with 1% osmium tetroxide, and stained with uranyl actetate (Farquhar and Palade, 1965). The pellets were dehydrated with ethanol, treated with propylene oxide, and embedded in Epon 812. Silver sections were stained with uranyl acetate and lead citrate (Reynolds, 1963).

For cryoimmunogold labeling of whole cells, cells were fixed in 3% paraformaldehyde/0.5% glutaraldehyde in 0.1 M cacodylate, pH 7.4. The cell wall of fixed cells was removed by incubation with 0.5 mg/ml zymolyase 20T (ICN) in 1.2 M sorbitol, 0.1 M phosphate-citrate, pH 7.0. Pellets were washed with 0.6 M sorbitol in the same buffer, embedded in 10% gelatin, and refixed as above. Pellets were infused with 2.3 M sucrose in PBS, and samples were frozen in liquid nitrogen until use (Tokuyasu, 1973). Ultrathin sections were made with glass knives in a Reichert-Jung FC-4E cryo-ultramicrotome. The sections were collected on Formvar-carbon coated nickel grids, treated with 1% BSA in PBS, and incubate with rabbit antithiolase (dilution = 1:5,000) or monoclonal 12CA5 antiserum against the HA-tag (dilution = 1:10). After buffer washes, the grids were incubated with goat anti-rabbit or anti-mouse IgG-gold (5 or 10 nm; Amersham Life Science, Arlington Heights, IL). The grids were processed and stained according to Griffiths et al. (1983).

For the immunolabeling of purified peroxisomes (see Fig. 11) and high salt-extracted peroxisomal membranes (see Fig. 3), the organelle or membrane pellets were fixed as described above, dehydrated in ethanol, and embedded in Lowicryl. Pale gold sections were collected on Formvar-carbon nickel grids. The sections were blocked with PBS containing 1% BSA and incubated with rabbit anti-Pox1p, anti-Fox3p (dilution = 1:5,000), or monoclonal 12CA5 antiserum against the HA-tag (dilution = 1:5). Characterization of the anti-Pox1p antibodies will be published elsewhere (Will G., and W. H. Kunau, personal communication). After washings, the grids were incubated with goat anti-rabbit or anti-mouse IgG-10 nm gold (Amersham) and stained with uranyl acetate.

Sections were viewed in an electron mnicroscope (100 CX; JEOL U.S.A. Inc., Peabody, MA) operated at 80 kV.
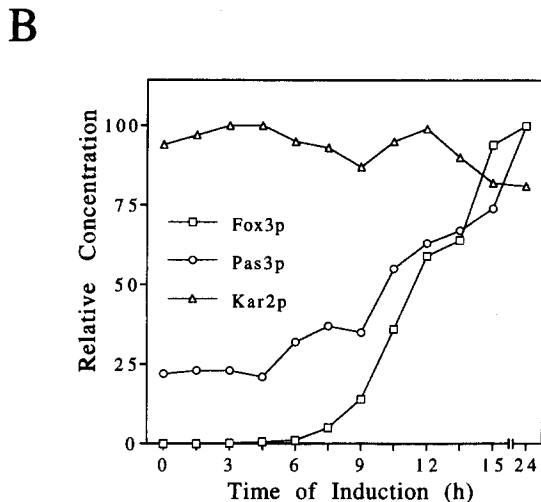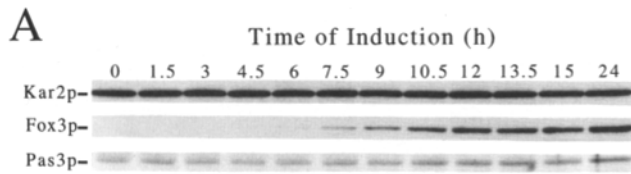
A

B

Figure 1. Time course of induction of a peroxisomal membrane protein *(Pas3p)* and a peroxisomal matrix protein *(Fox3p)*. Cells were shifted to oleic acid–containing medium and were cultured for the indicated time points. (*A*) Whole-cell extracts were prepared for SDS-PAGE and Pas3p, Fox3p, and Kar2p (a marker for the endoplasmic reticulum; Rose et al., 1989) were detected by immunoblot analysis. The amounts analyzed were 1% of the homogenates from 30 mg of cells. (*B*) Relative concentrations of the proteins as determined by laser densitometry of the immunoblot data. The concentration at 24 h postinduction was set at 100%.

Immunoblots

Western blot analysis was performed according to standard protocols (Towbin et al., 1979) using anti–rabbit or anti–mouse IgG–coupled HRP as second antibody (Amersham). Protein–antibody complexes were visualized by treatment with HRP chemoluminescence developing reagents (ECL system; Amersham). Western blots were quantitated by laser densitometry. Polyclonal rabbit antibodies against Fox3p (Erdmann and Kunau, 1994), Kar2p (Rose et al., 1989), and p32 (Pain and Blobel, 1990) were used at dilutions of 1:50,000. Pas3p was detected with a nondiluted affinity-purified rabbit antiserum against the protein (Höhfeld et al., 1991). HA-tagged Pmp27p

was detected with monoclonal 12CA5 antiserum against the HA-Tag (BAbCO; dilution = 1:3,000).

Analytical Procedures

Catalase (EC 1.11.1.6) was assayed according to Moreno de al Garza et al. (1985). Protein was measured by laser densitometry of proteins separated by SDS-PAGE and stained with Coomassie blue, as well as by the method of Bradford (1976) with bovine serum albumin as standard.

Results

Oleate Induction of Peroxisomal Proteins

S. cerevisiae cells were shifted from growth in glucose-containing media to growth in oleate-containing media. At various time points, cell homogenates were prepared, and the proteins were separated by SDS-PAGE, transferred to nitrocellulose, and probed with antibodies against either Pas3p (a peroxisomal membrane protein), Fox3p (a peroxisomal matrix protein), or Kar2p (a matrix protein of the endoplasmic reticulum) (Fig. 1). Even before shift to oleate-containing media, cells contained readily detectable levels of Pas3p (Höhfeld et al., 1991; Fig. 1, lane *1* in this manuscript), whereas Fox3p was not detectable (Fig. 1, lane *1*). During a 24-h induction period, Pas3p increased about four to fivefold, whereas Fox3p increased from nondetectable to clearly detectable levels (Fig. 1). The levels of Kar2p, serving as a control, remained essentially unchanged during the 24-h induction period.

Peroxisome Induction Causes Shift of Pas3p from Light to Heavy Membranes

As Pas3p could be used as a peroxisomal membrane marker that is detectable in noninduced cells, it became possible to assess physical characteristics of the peroxisomes before and after various times of induction. This was done by gradient centrifugation of postnuclear supernatants of cell homogenates. We found that before induction, most of the Pas3p-reactive membranes banded at a density of 1.15 g/ml (Fig. 2, fraction *11*). At the 3-h point, the bulk of Pas3p-reactive membranes shifted to a broad band of higher density between 1.16 and 1.20 g/ml. (Fig. 2). This bulk shift to higher density continued at the 6-h point, and it was completed at the 12-h point when the bulk of the Pas3p-reactive membrane equilibrated at 1.21 g/ml (Fig. 2, fraction *3*). However, a fraction of the Pas3p- reactive membrane remained at 1.15 g/ml and at the broad region between 1.15 and 1.21 g/ml (this was clearly evident after overexposure of the
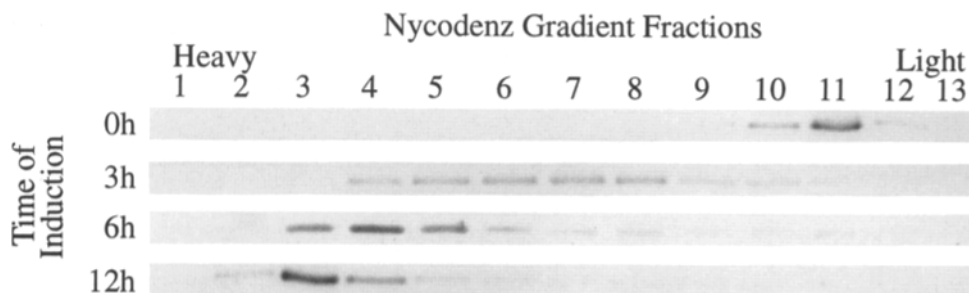

Figure 2. Isopycnic gradient centrifugation analysis of Pas3p reactive membranes of cells shifted to oleate containing media and cultured for the indicated times. Cell homogenates were fractionated on continuous 15–35% Nycodenz gradients (see Materials and Methods), and gradient fractions were analyzed by immunoblots with αPas3p. Fraction

numbers are indicated and each lane corresponded to 1.25% of the fraction volume. Peroxisomes from noninduced cells peaked at a density of 1.15 g/cm³ (fraction 11), but at later stages of induction, peroxisomes were mainly obtained at 1.21 g/cm³ (fraction 3).
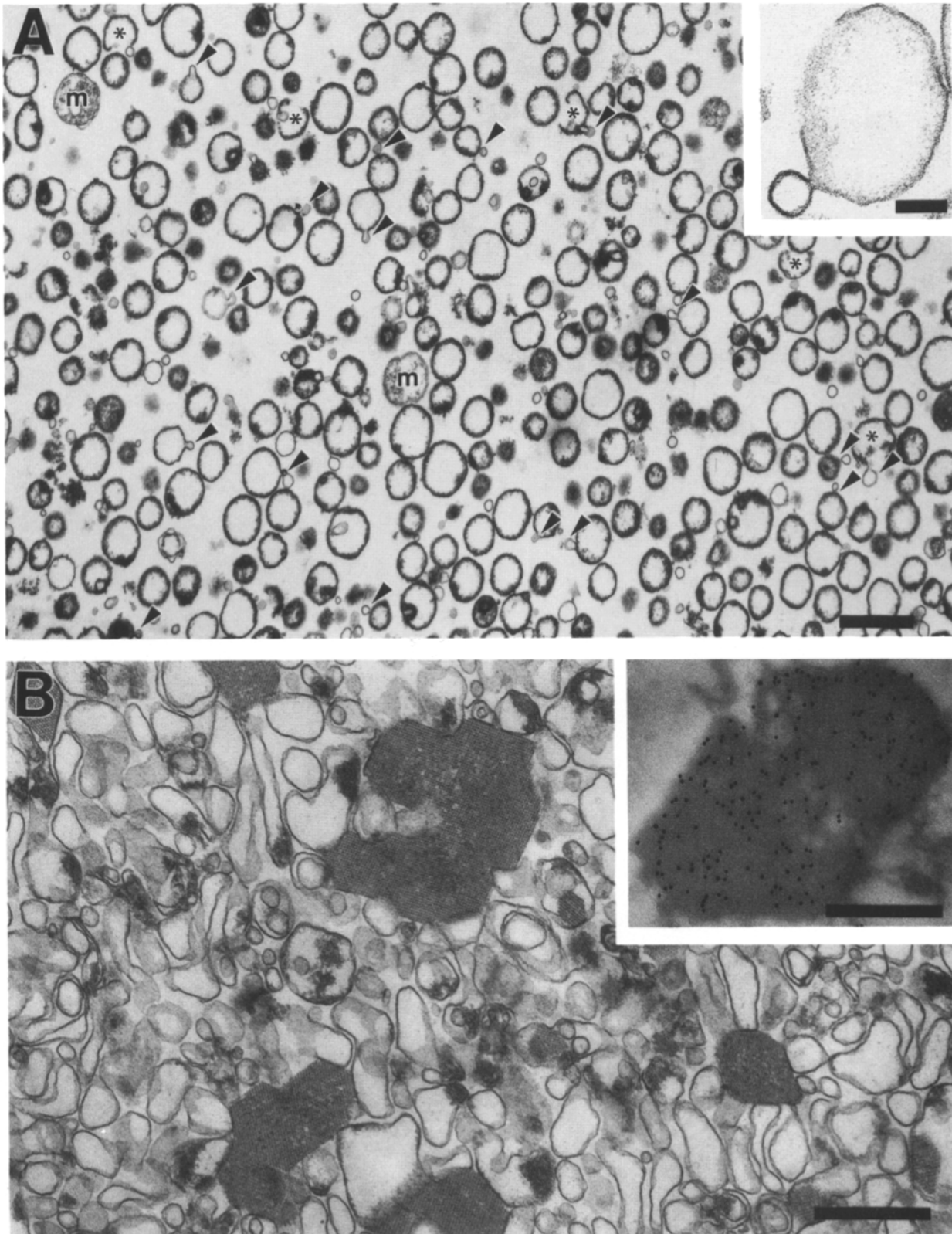
Figure 3. Electron microscopy of isolated peroxisomes before (*A*) and after (*B*) extraction with high salt. (*A*) The ultrastructural appearance of purified peroxisomes from *S. cerevisiae* that had been induced for 9 h on oleic acid medium is characterized by the presence of finger-like membrane extensions (*black arrowheads*). Some of the peroxisomes appear to be broken (*asterisks*). Few mitochondria (*m*) were found in the preparation. A higher magnification of a peroxisome is shown in the inset, showing the continuity of the peroxisomal membrane between the bulbous peroxisome and its extended domain. Bars, 1 µm and 0.1 µm (*inset*). (*B*) Ultrastructural appearance of acyl-CoA oxidase crystals in "high salt"–extracted peroxisomal membranes (see Materials and Methods). The inset shows the localization of acyl-CoA oxidase within the crystals by immunoelectron microscopy. Sections were probed with a polyclonal antibody against the acyl-CoA oxidase from *S. cerevisiae* and goat anti–rabbit antibodies coupled to 10 nm gold. Bars, 0.5 µm.

blot in Fig. 2 (data not shown). Thus, in noninduced cells, the bulk of the Pas3p-reactive peroxisomes consisted of light membranes (comparable to smooth endoplasmic reticulum derived membranes).

Purification of Peroxisomes

A 9-h point of induction was chosen for the isolation of peroxisomes since this was about the earliest time point at which the bulk of the Pas3p-reactive membranes had shifted to the heavy density of 1.21 g/ml (Fig. 2). Only these dense membranes can be expected to be readily separable from mitochondria and ER membranes.

Using two consecutive gradient centrifugation procedures (see Materials and Methods), we obtained highly purified peroxisomes (Fig. 3 A). Much of the peroxisomal matrix was lost since most peroxisomes appeared empty. By electron microscopy, some peroxisomes appear broken and unsealed (Fig. 3 A); however, two ultrastructural features stand out. First, there is the presence of a dense cortical layer of material apposed to the lumenal side of the peroxisomal membrane (Fig. 3 A). This cortical layer may represent some organization of the peripheral matrix with respect to the peroxisomal membrane, and it could be the principal reason for the high density of the isolated peroxisomes in spite of the apparent loss of a fraction of matrix proteins. Second, finger-like membrane extensions and small vesicles were often associated with the peroxisomal membrane (Fig. 3 A). In favorable sections, the attached small vesicle membrane is continuous with the peroxisomal membrane (Fig. 3 A, inset). Moreover, the membrane of the attached vesicles does not contain the dense cortical layer that is characteristically apposed only to the bulbous peroxisomes. We believe that these smooth surfaced vesicles are remnants of tubular extensions of the peroxisomal membrane that were not sheared off during the homogenization and gradient centrifugation procedures and that, therefore, copurified with the bulbous peroxisomes.

Extraction of Purified Peroxisomes; Subfractionation of Integral Membrane Proteins

The purified peroxisomes were consecutively extracted at low salt, high salt, and at pH 11.0 (see Materials and Methods). The proteins of the starting material, the various extracts, and the remaining membranes were separated by SDS-PAGE, and they were visualized by Coomassie blue staining (Fig. 4 A). Most of the major proteins of the peroxisomal membranes were extracted, some at low salt and others at high salt (Fig. 4 A). These proteins are likely the components of the dense cortical layer aassociated with the peroxisomal membrane (see Fig. 3). Immunoblot analysis (Fig. 4 B) showed that Fox3p was among the extracted matrix proteins (Fig. 4 B). However, one of the major peroxisomal proteins, identified as acyl-CoA oxidase (Poxlp, Dmochowska et al., 1990) by peptide sequencing (data not shown), was only partially extracted by high salt, most likely as a result of extraction-induced formation of paracrystals (Fig. 3 B). As expected, the integral membrane protein Pas3p remained associated with the membrane, even after alkali extraction (Fig. 4 B).

Electron microscopic analysis of the high salt extracted membranes showed the presence of largely smooth membranes (Fig. 3 B) without the dense cortical layer that is
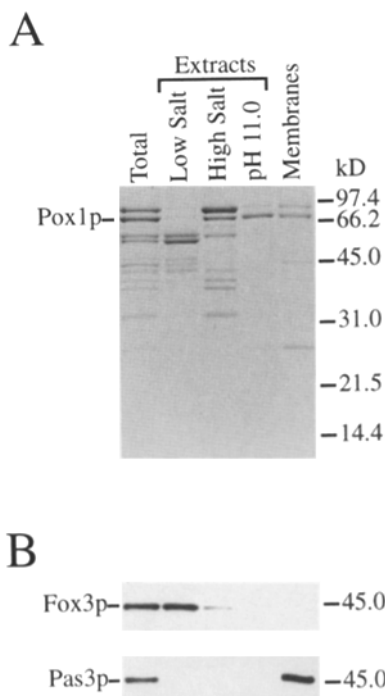

Figure 4. Successive extraction of peroxisomes and immunological detection of peroxisomal marker proteins in subfractions. (A) Coomassie stain of total peroxisomal proteins (lane 1) and proteins of peroxisomal subfractions obtained by successive treatment of total purified peroxisomes with low salt, high salt, and pH 11.0 (see Materials and Methods). Lane 5 shows the protein content of the final membrane pellet. (B) Immunological detection of the peroxisomal matrix marker Fox3p and the peroxisomal membrane marker Pas3p by Western blot analysis of the subfractions. The amount of the peroxisomal subfractions loaded in lanes 2–5 corresponded to four equivalents of the total peroxisomal protein in lane 1.

characteristic of nonextracted peroxisomes (Fig. 3 A). However, some of the membranes were assocaited with striking paracrystalline structures that must have formed during extraction (Fig. 3 B). These paracrystalline structures contain Poxlp as shown by immunogold labeling (Fig. 3 B, inset).

High salt extracted peroxisomal membranes were solubilized in SDS and the proteins separated by HPLC. Proteins in various HPLC fractions were separated by SDS-PAGE and visualized by Coomassie blue (Fig. 5). About 30 distinct polypeptides can be discerned. One of the major proteins of an apparent molecular mass of 27 kD (Fig. 5) was subjected to partial protein sequencing in preparation for DNA cloning and sequencing of the corresponding PMP27 gene (see Materials and Methods).

DNA-deduced Primary Structure of Pmp27p

The PMP27 open reading frame encodes a polypeptide of 236 amino acid residues with a calculated molecular mass of 26,879 D (Fig. 6 A) in good agreement with the molecular mass estimated by SDS-PAGE (Fig. 5). Hydrophilicity plots according to Kyte and Doolittle (1982) revealed several hydrophobic regions, but none of them appeared to fulfill the requirements for a membrane spanning α helix (data not shown). However, using a manual β turn identification pro-
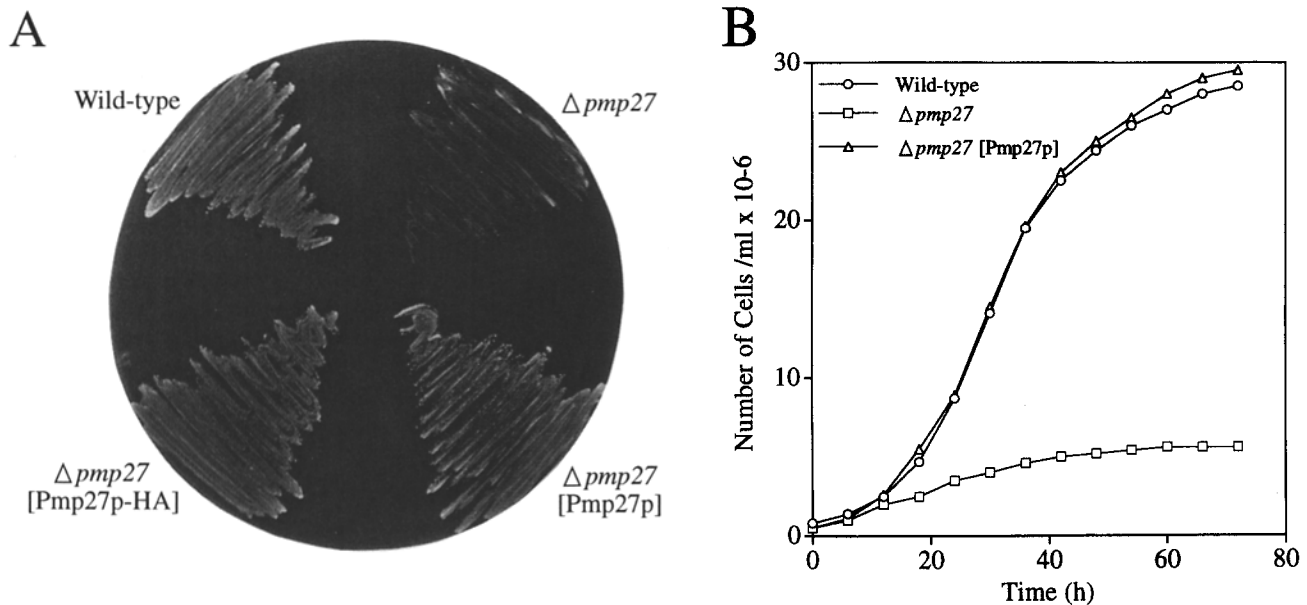
HPLC Fractions

36 37 38 39 40 41 42 43 44 45 46 47 48 49 50 51 52 53 54 55 56 57 58 59 60 61 62 63 64 65 66 67 68

Figure 5. Preparative chromatographic separation of peroxisomal membrane proteins. High salt–extracted peroxisomal membranes (1 mg protein) were solubilized in SDS and separated by reverse phase HPLC (see Materials and Methods). Polypeptides of selected fractions were separated by SDS-PAGE and visualized by Coomassie blue staining. The position of Pmp27p is indicated by an arrowhead. The position of acyl-CoA oxidase, identified by peptide sequencing (data not shown), is marked by an asterisk. The amount per lane corresponded to 12.5% of the total fraction.

A

cedure (Paul and Rosenbusch, 1985) and on the assumption that the bulk of PMP27p is embedded in the bilayer, Pmp27p could have as many as nine transmembrane segments (data not shown). Pmp27p contains none of the peroxisomal targeting signals that have so far been identified (Gould et al., 1989; Swinkels et al., 1991; Aitchison et al., 1991; Subramani, 1992).

A search of the database revealed similarity to two peroxisomal membrane proteins (PMPs) of *C. biodinii*, termed PMP31 and PMP32 (Moreno et al., 1994). cbPMP31 and cbPMP32 are 92% identical and scPmp27p is 32% identical to cbPMP31 (Fig. 6 *B*). Thus scPmp27p could be the *S. cerevisiae* homologue of cbPMP31/cbPMP32.

Pmp27p is Essential for Growth on Oleate

One genomic copy of *PMP27* in the diploid wild-type W303 was replaced with *LEU2*. The proper integration of the deletion construct into the genome was confirmed by Southern blotting (data not shown). Tetrad analysis showed a 2:2 segregation for Leu+. All spores derived from the tetrads were viable, indicating that Pmp27p is not essential for growth on YPD medium. However, on oleic acid medium, a 2:2 segregation for growth ability was observed. The growth defect on oleic acid medium cosegregated with the Leu+ marker, therefore indicating that the *PMP27* gene product is essential for growth on oleic acid medium. However, Δpmp27 mutant cells grew normally on ethanol medium (data not shown). The imparied growth phenotype on oleate of a haploid Δpmp27 strain, derived from this tetrad analysis, is shown in Fig. 7 *A*. Δpmp27 cells regained

B

Figure 6. Nucleotide and deduced amino acid sequence of the *S. cerevisiae PMP27* locus (*A*) and comparison with PMP31 from *C. boidinii* (*B*). (*A*) A putative oleic acid responsive element (Einerhand et al., 1993) and a presumptive TATA sequence (Struhl, 1987) in the 5′ noncoding region, as well as presumptive termination sequences in the 3′ noncoding region (Zaret and Sherman, 1982), are underlined. The underlined amino acid sequence was obtained by peptide sequencing of the purified Pmp27p. (*B*) Identical residues are indicated by vertical bars. Two dots represent similar residues. The identity betwen both proteins is 32%, and the similarity 59%. Similarity rules: G=A=S, P=A=S, S=T=A, D=E=Q=N, K=R, V=I=L=M=F, F=Y. These sequence data are available from EMBL/GenBank/DDBJ under accession No. X81465.

Figure 7. Pmp27p is essential for growth on oleic acid medium. (*A*) Wild-type W303a, Δ*pmp27* mutant, and Δ*pmp27* mutant cells expressing Pmp27p or HA-tagged Pmp27p from single-copy plasmids were plated on oleic acid medium and incubated for 7 d at 30°C. (*B*) Growth curve of wild-type, Δ*pmp27*, and complemented Δ*pmp27* in oleic acid liquid culture. The growth defect of the Δ*pmp27* mutant becomes obvious after 12 h, when wild-type and the complemented strain enter the logarithmic growth phase. At this timepoint, the growth of the mutant ceased.

the ability to grow on oleic acid medium when transformed with the wild-type copy of *PMP27* (Fig. 7 *A*). The growth defect of Δ*pmp27* could also be complemented by expression of a tagged Pmp27p-HA, indicating that the tagging had no obvious effect on the function of the protein (Fig. 7 *A*). Fig. 7 *B* shows the rate of growth of the various strains after transfer from glucose-containing media to oleate-containing media. Complemented Δ*pmp27* cells grew as well as wild-type cells, whereas mutant Δ*pmp27* cells ceased to grow after transfer to oleate.

Immunolocalization of Pmp27p

The cellular location of epitope-tagged Pmp27p (Pmp27p-HA) was examined by immunofluorescence microscopy, immunoblot analysis of subcellular fractions, and immunoelectron microscopy. The tag, which consisted of a 10–amino acid epitope derived from the hemagglutinin antigen (HA), was introduced at the extreme COOH terminus of Pmp27p. The tagged protein was expressed in Δ*pmp27* cells, which contain a chromosomal disruption of the wild-type *PMP27* gene (see Materials and Methods). Expression of the tagged Pmp27p was under the control of its own promoter on a single-copy plasmid. As expression resulted in functional complementation of the mutant phenotype of Δ*pmp27* (see Figs. 7, 12, and 14), the tagging apparently did not influence the function of Pmp27p. Thus, subcellular localization of the tagged Pmp27p can be expected to closely mirror that of wild-type Pmp27p.

The HA-tagged Pmp27p was readily identified among the SDS-PAGE–separated polypeptides of a total homogenate of cells grown for 12 h in oleate containing medium with αHA monoclonal antibodies (Fig. 8 *A*).

To examine whether *PMP27* expression is induced by growth in oleate-containing medium, cells were grown on

low glucose medium and were subsequently shifted to oleate containing medium. At various time points, cell homogenates were prepared and analyzed by immunoblotting with αHA mAbs and αFox3p. Pmp27p was found to be highly inducible by oleate (Fig. 8 *B*) and its induction appeared to precede that of Pox3p by 1–2 h (Fig. 8 *B*). All further analyses were done with cells at the 12-h time point of induction.

Double immunofluorescence microscopy using αFox3p and αPmp27p-HA showed an identical staining pattern, demonstrating that Pmp27p is a peroxisomal protein (Fig. 9).
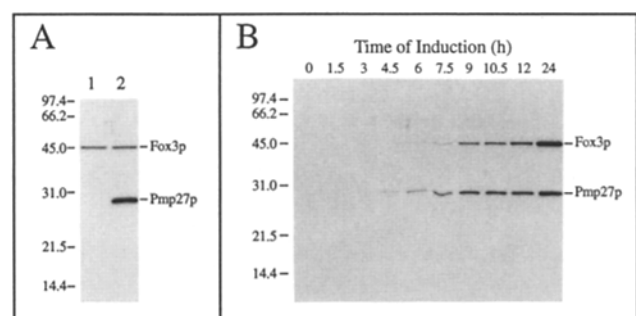

Figure 8. Immunological detection of HA-tagged Pmp27p (*A*) and time course of Pmp27p induction by oleic acid (*B*). (*A*) Equal amounts of whole-cell lysates from oleic acid induced Δ*pmp27* cells expressing Pmp27p (lane *1*) and HA-tagged Pmp27p (lane *2*) were subjected to Western blot analysis with rabbit antiserum against Fox3p and mAb against the HA-tag (see Materials and Methods). The amount loaded per lane corresponds to 0.5% of extracts from 30 mg of cells. (*B*) Δ*pmp27* [Pmp27p-HA] cells expressing the HA-tagged Pmp27p were shifted to oleic acid containing medium. At indicated timepoints, whole-cell extracts were prepared and subjected to Western blot analysis with mAb against the HA-tag.
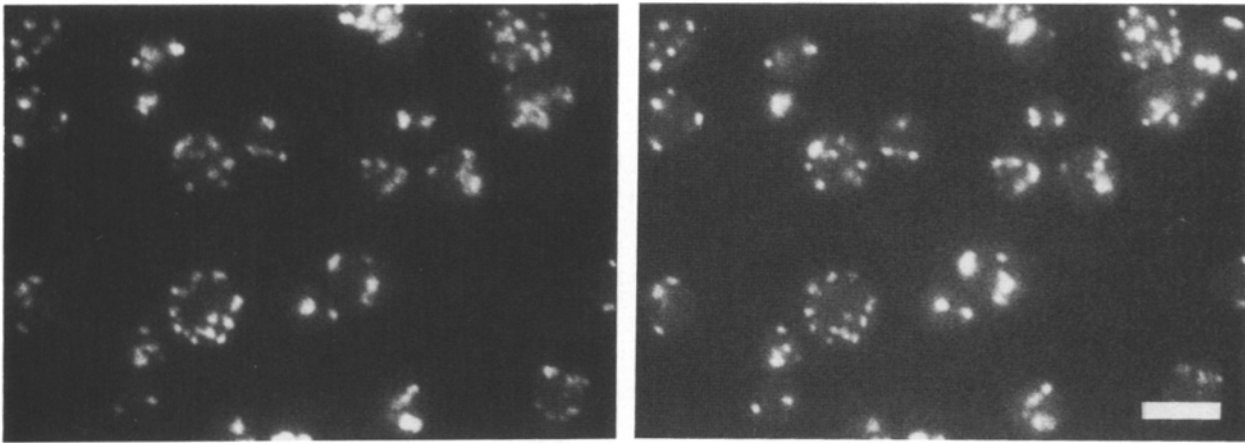
anti-HA-Pmp27p · · · anti-thiolase

Figure 9. Double immunofluorescence microscopy localition of Fox3p and HA-tagged Pmp27p. Oleic acid induced Δ*pmp27* cells expressing the HA-tagged Pmp27p were processed for double immunofluorescence microscopy using mAb against the HA-tag (*anti-Pmp27p-HA*) and a rabbit antibody against peroxisomal thiolase (*anti-thiolase*). Secondary antibodies were FITC-conjugated anti-mouse IgG and Texas red-conjugated anti-mouse IgG. Bar, 5 μm.

Immunoblot analyses of cell fractions that were obtained by differential centrifugation of a homogenate are shown in Fig. 10 *A*. Although most of the Pmp27p-HA–reactive membranes that were present in a postnuclear supernatant (lane *1*) sedimented at 25,000 *g* (lane *3*), a significant amount remained in the corresponding supernatant (lane *2*). This latter material may represent tubular membranes that were sheared off from the peroxisomal membrane during homogenization. The membranes that were pelleted at 25,000 *g* were resuspended and further fractionated by sucrose gradient centrifugation. Immunoblot analysis of fractions probed with αHA, αFox3p, and αp32 (p32 being a mitochondrial marker) is shown in Fig. 10 *B*. As expected for peroxisomal components (see Fig. 2), most of the αPmp27p-

HA– and αFox3p-reactive membranes peaked at a density of 1.21 g/ml (Fig. 10 *B*, fraction *9*) clearly separated from mitochondria that peak at a density of 1.17 g/ml (Fig. 10 *B*, fraction *17*). However, a significant amount of the αPmp27p-HA–reactive membranes banded at lighter densities (Fig. 10 *B*). Again, these lighter membranes could be derived from tubular membranes sheared off from the peroxisomes.

Pmp27p-HA that is associated with the purified membrane fraction behaves as an integral membrane protein since most of it was not extracted at pH 11.0 (Fig. 10 *C*).

Immunoelectron microscopy of isolated peroxisomes using αPmp27p-HA showed gold labeling of the peroxisomal periphery consistent with Pmp27p being a peroxisomal membrane protein (Fig. 11 *A*). Immunoelectron microscopy
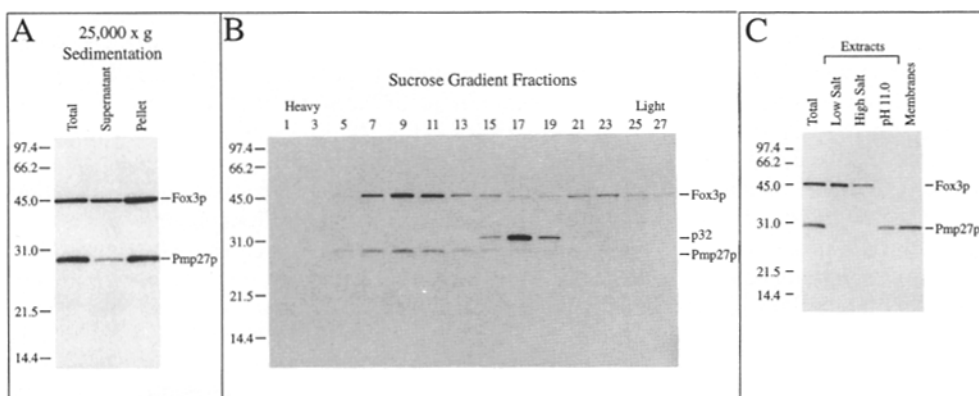

Figure 10. Coenrichment of HA-tagged Pmp27p and peroxisomal thiolase during peroxisome isolation (*A* and *B*) and intraperoxisomal localization of Pmp27p-HA (*C*). (*A*) Immunoblot analysis of cell fractions that were obtained by differential centrifugation (see Materials and Methods) of the cell homogenate from oleic acid induced Δ*pmp27* cells expressing the HA-tagged Pmp27p. (*B*) The organelles of the 25,000-g pellet were separated on a 36–68% (wt/vol) sucrose gradient (see Materials and Methods). 1.2-ml fractions were collected from the bottom of the gradient. Localization of HA-Pmp27p, as well as peroxisomal thiolase and mitochondrial p32 (Pain et al., 1990), in fractions was monitored by immunoblot analysis. Peroxisomes peaked in fraction 9 at a density of 1.23 g/cm³. Mitochondria peaked in fraction 17 at a density of 1.17 g/cm³. Pmp27p-HA as well as Fox3p were mainly found in the peroxisomal peak fractions. (*C*) The isolated peroxisomes (fraction 9 in *B*) were extracted by low salt, high salt, and pH 11.0 treatments (see Materials and Methods). As most of the Pmp27p-HA was not extracted by either means (lane *5*), it behaves as an integral membrane protein. Equivalent amounts of proteins were loaded per lane. HA-Pmp27p and thiolase amounts in peroxisomal subfractions were monitored by Western blot analysis (see Materials and Methods).
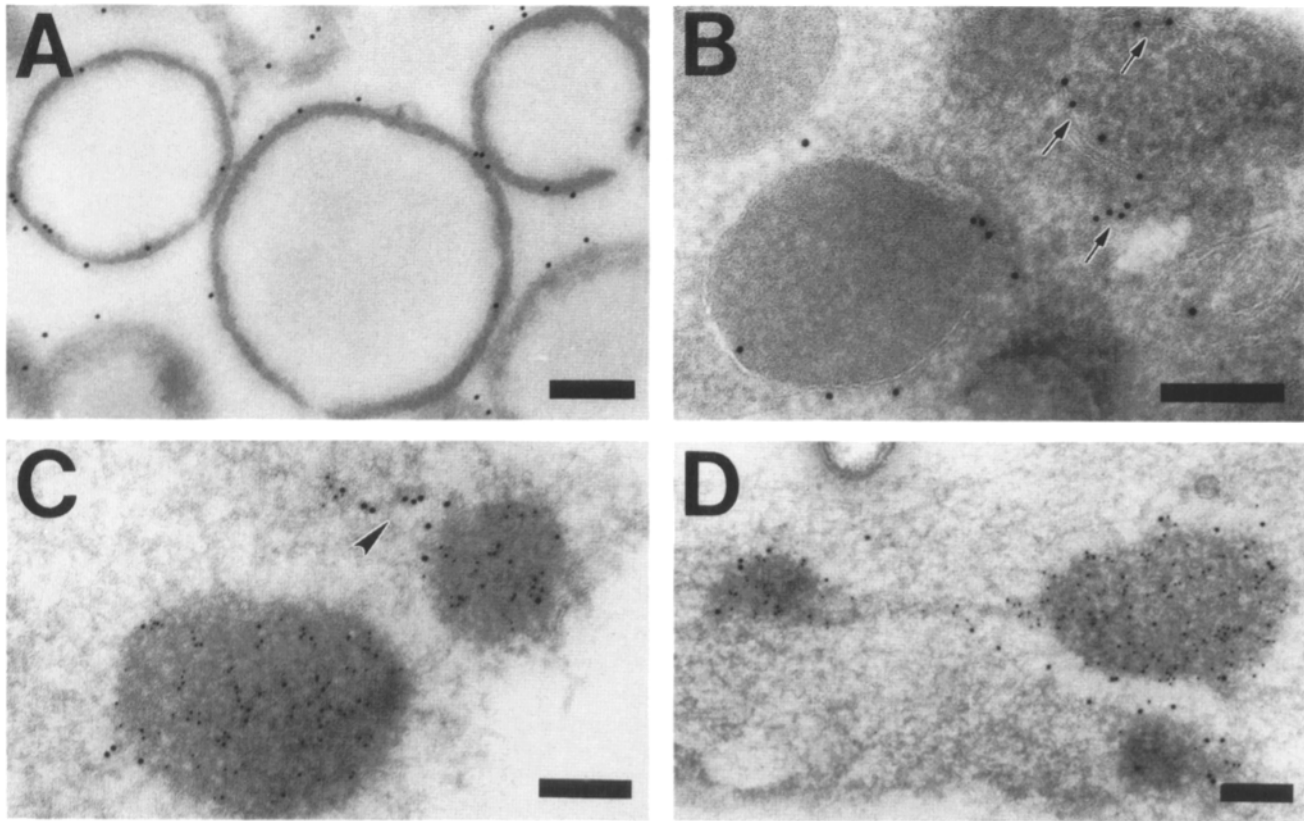
Figure 11. Immunoelectron microscopy localization of Pmp27p in isolated peroxisomes (*A*) and 12 h oleic acid induced Δ*pmp27* cells expressing the HA-tagged Pmp27p (*B*). A double labeling of the cells for thiolase (5 nm gold) and Pmp27p (10 nm gold) localization is shown in (*C* and *D*). (*A*) Immunogold labeling of the peroxisomal periphery is consistent with Pmp27p being a peroxisomal membrane protein. (*B*) Pmp27p was found to be associated with the peroxisomal membrane, but additional labeling of membrane loops or tubules was frequently found in the proximity of peroxisomes (black arrows). (*C*) Double labeling showed Pmp27p labeling of thiolase-negative membrane structures extending from the spherical peroxisomes (*black arrowhead*). (*D*) Interconnection of bulbous peroxisomes by a thiolase-containing tubular region. Localization of the HA-tagged Pmp27p was monitored with mAb against the tag, and thiolase was localized with rabbit antibody against the protein. Isolated peroxisomes were from 9 h oleic acid induced Δ*pmp27* cells expressing HA-tagged Pmp27p. Bars, 0.2 μm.

of frozen thin sections of spheroplasts using α Pmp27p-HA showed gold labeling in the peroxisomal periphery, as expected for a membrane protein (Fig. 11 *B*). However, there also was gold labeling of a region in the vicinity of the peroxisomes that coincided with tubular membrane loops (Fig. 11 *B, black arrows*). Double immunoelectron microscopy of frozen thin sections of cells using αPmp27p-HA (10 nm gold) and αFox3p (5 nm gold) showed the expected gold labeling of the peroxisomal membrane and the peroxisomal matrix, respectively (Fig. 11 *C*). In addition, there was labeling with only 10 nm gold (Fig. 11 *C, black arrowheads*) in what appear to be matrixless, peroxisome-attached tubules. In some sections, an interconnection of bulbous peroxisomes by a tubular matrix–containing region could be detected (Fig. 11 *D*).

Morphological Characterization of Δpmp27 Cells

Immunofluorescence microscopy using α Fox3p was done with methanol-fixed spheroplasts of wild-type cells, Δ*pmp27* cells, and Δ*pmp27* cells complemented with a copy of the wild-type *PMP27* gene (Fig. 12). Analysis was after cells were shifted to growth in oleate-containing media for a period of 0–24 h. When induced for 12 h, in wild-type

spheroplasts, a characteristic punctate pattern of 10–20 small spots was observed. (Fig. 12 *A, upper panel*). In the mutant Δ*pmp27* cells, however, there was a striking reduction in the number of spots with a considerable increase in the size of the individual spots (Fig. 12 *A, middle panel*). Complementation of the mutant cells with the wild-type gene gave a pattern (Fig. 12 *A, lower panel*) indistinguishable from that of wild-type cells (Fig. 12 *A, upper panel*). A time course of oleic acid induced peroxisome proliferation of Δ*pmp27* cells and complemented mutant cells is shown in Fig. 12 *B*. Peroxisomes were detected in both strains, even from the very beginning of induction, and no significant difference with respect to the size and number of detected organelles was observed (Fig. 12 *B, 0 and 3 h*). However, as early as 6 h after the start of induction, the mutant phenotype, indicated by fewer but bigger peroxisomes, became obvious. Most striking was the difference at later stages of induction, when the complemented strain was filled with small dots, but only one to a few giant peroxisomes were detected in the Δ*pmp27* mutant cells (Fig. 12 *B, 24 h*).

Electron microscopy (Fig. 13, *A* and *B*) and immunoelectron microscopy (Fig. 13, *C* and *D*) of thin sections of Δ*pmp27* mutant cells and complemented Δ*pmp27* cells using
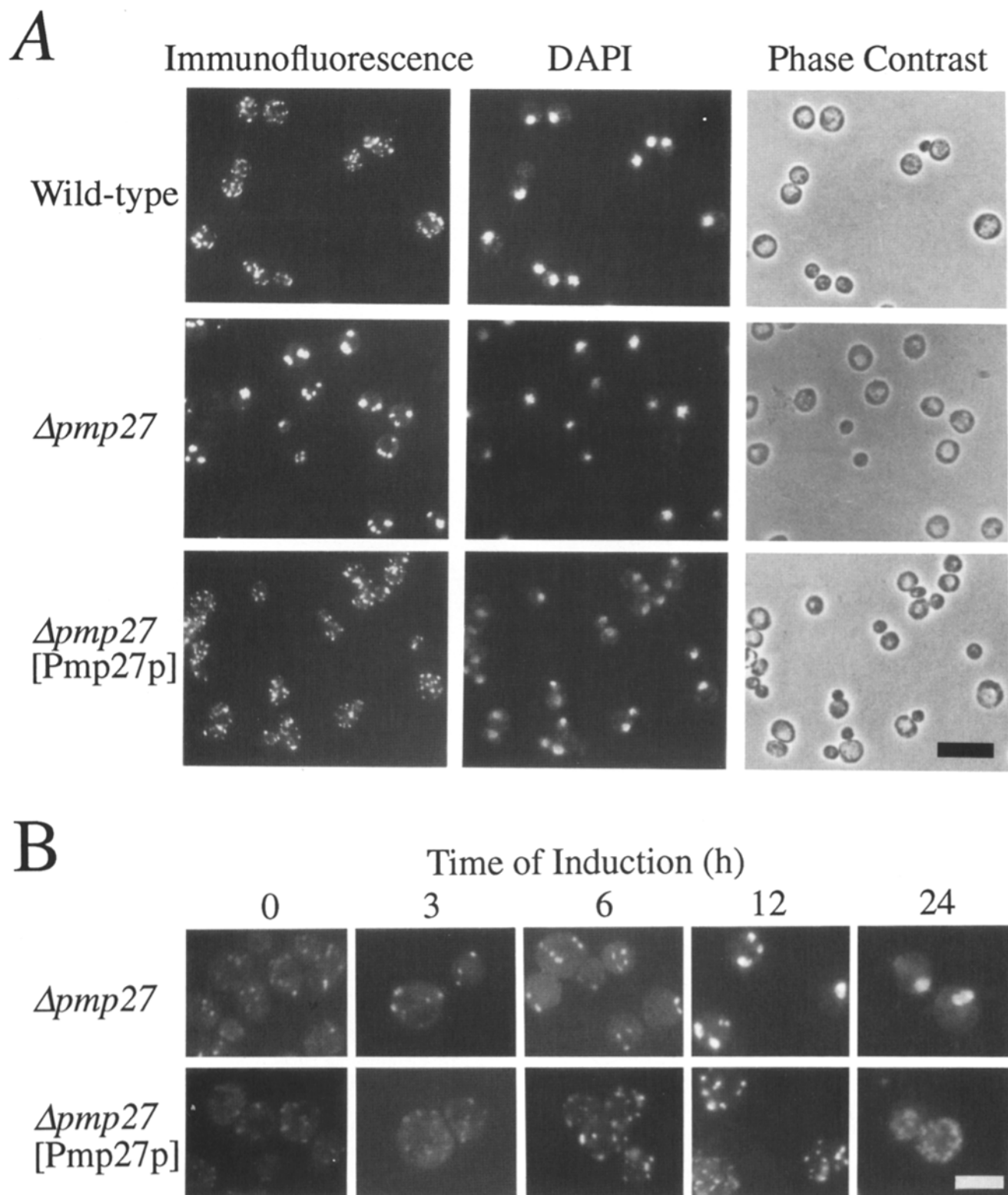
Figure 12. Immunofluorescence microscopy localization of thiolase in wild-type, Δ*pmp27* mutant, and Δ*pmp27* mutant cells expressing Pmp27p. (*A*) Cells were induced for 12 h on oleic acid medium. The panels show either thiolase localization by immunofluorescence, DAPI staining of DNA by fluorescence, or phase contrast micrographs of the same cells. Bar, 10 μm. (*B*) Comparison of oleic acid induced peroxisome proliferation in Δ*pmp27* mutant and Δ*pmp27* mutant cells expressing Pmp27p. Thiolase localization was determined using a polyclonal antiserum against the enzyme and Texas red–labeled donkey anti–rabbit antiserum. Bar, 5 μm.
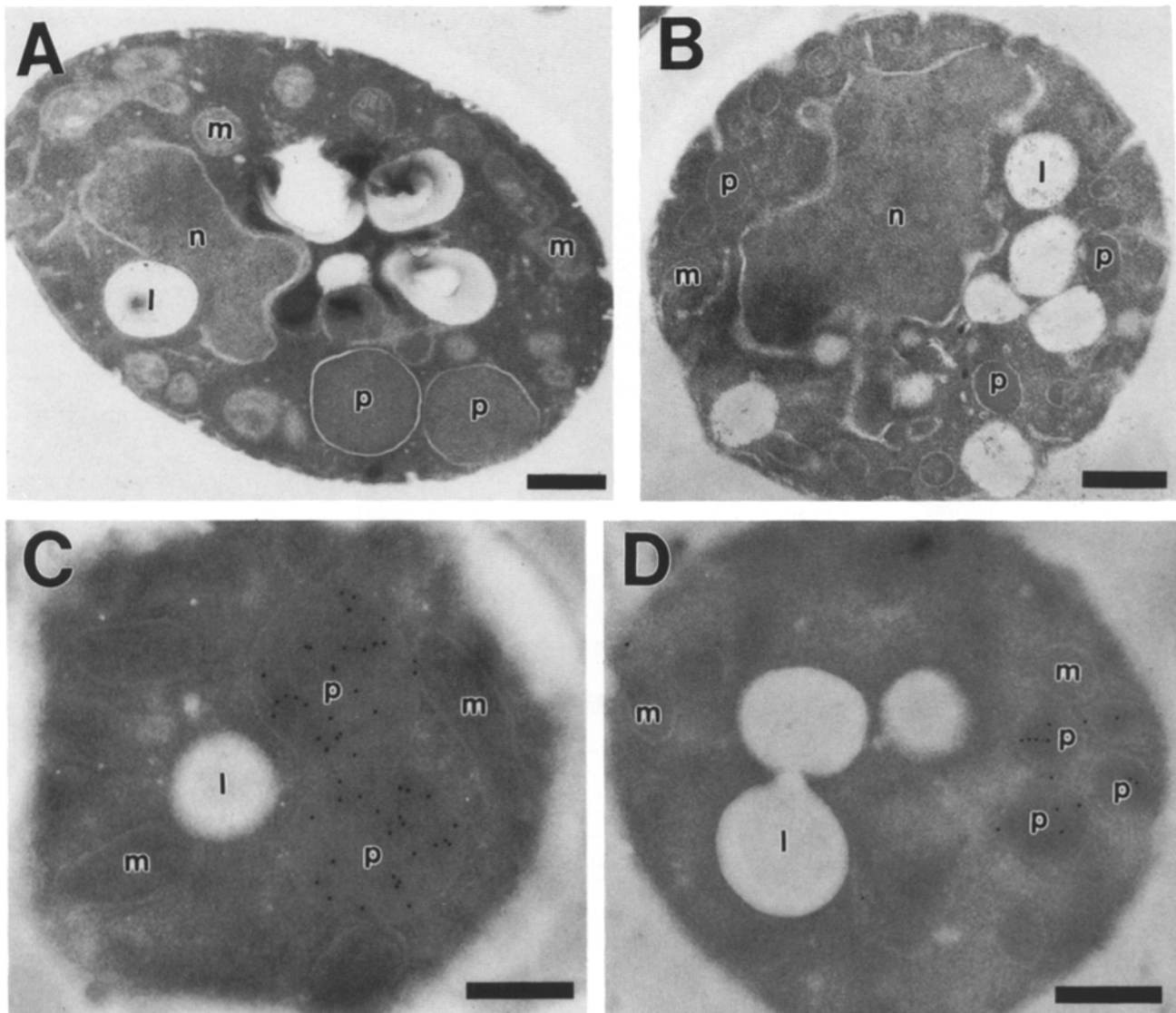
Figure 13. Electron microscopy (*A* and *B*) and immunoelectron microscopy (*C* and *D*) of 12-h oleic acid–induced Δ*pmp27* mutant cells (*A* and *C*) and complemented Δ*pmp27* cells (*B* and *D*). The mutant phenotype (*A* and *C*) was characterized by the presence of fewer, but larger peroxisomes. Sections were probed with polyclonal antiserum against thiolase and goat anti–rabbit antibodies coupled to 10 nm gold. *p*, peroxisome; *m*, mitochondrion; *n*, nucleus; *l*, lipid droplet. Bars, 0.5 μm.

α Fox3p confirmed the immunofluorescent images of Fig. 12. Peroxisomes in the mutant cells were considerably larger and less abundant than those in the complemented strain.

Δpmp27 Cells Are Defective in Peroxisomal Inheritance

Δ*pmp27* cells cultured in oleic acid liquid medium showed multiple buds (Fig. 14). Electron microscopical investigation of these cells showed that giant peroxisomes could easily be detected in the majority of mother cells but no peroxisomes were found in cell buds. Other cell organelles (mitochondria, nuclei) showed normal morphology, and they were nearly always detected in the buds (data not shown). Immunofluorescence microscopy of the mutant cells incubated for 48 h in oleic acid medium showed the presence of one to a few giant peroxisomes in mother cells and confirmed the absence of peroxisomes in virtually all cell buds (Fig. 15).

Discussion

We have identified an integral membrane protein, Pmp27p, of *S. cerevisiae* peroxisomes. This protein served as a membrane marker for immunoelectron microscopy analysis of the peroxisomal compartment of *S. cerevisiae*, providing evidence for the existence of tubular extensions of the peroxisomal membrane. Yeast cells lacking Pmp27p possess giant peroxisomes, and they are defective for peroxisomal inheritance.

Pmp27p is only the second integral membrane protein of *S. cerevisiae* that has been molecularly cloned and sequenced, Pas3p (Höhfeld et al. 1991) being the first. In peroxisomal membranes that were purified from cells induced for peroxisome proliferation by growth on oleate, Pmp27p was the most abundant peroxisomal membrane protein (Fig. 5). Analysis of its DNA-deduced primary structure did not yield any clues as to its function. So far we have no
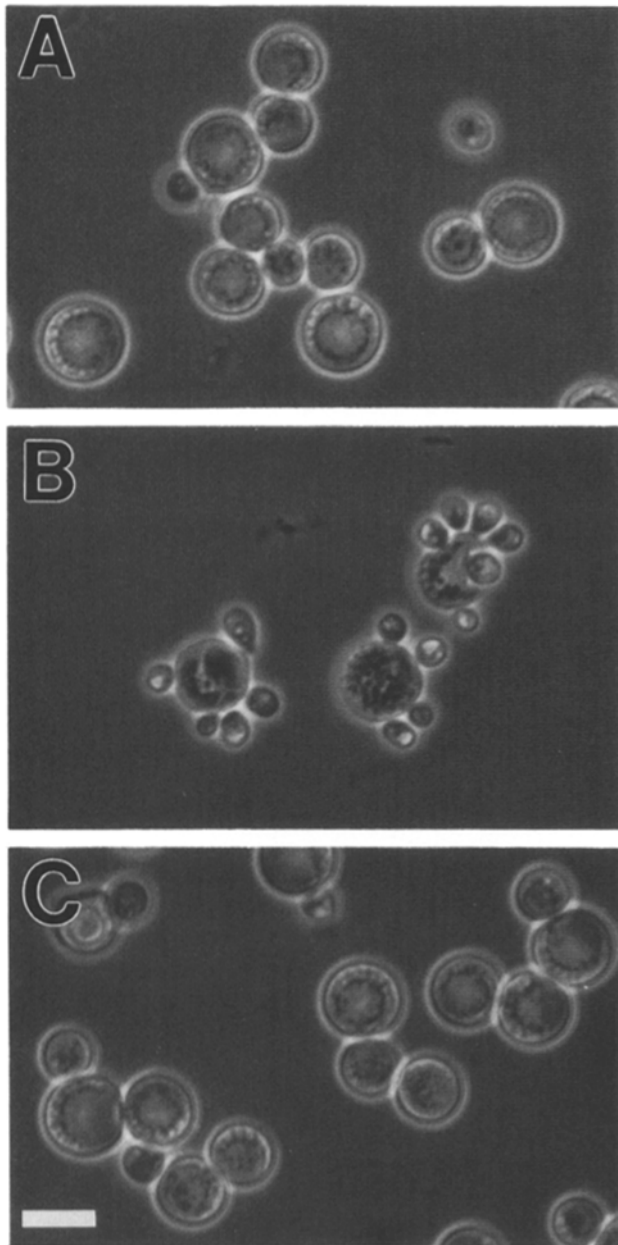
Figure 14. Multiple buds in Δ*pmp27* mutant cells after long-term incubation in oleic acid medium. Phase contrast micrographs of W303a wild-type cells (*A*), Δ*pmp27* mutant cells (*B*), and complemented Δ*pmp27* cells (*C*) incubated for 5 d in oleic acid liquid medium. Bar, 5 μm.

data on the topology of Pmp27p in the peroxisomal membrane. Searches in the data banks showed similarity to two integral peroxisomal membrane proteins of *C. biodinii*, PMP31 and PMP32 (Moreno et al., 1994). It remains to be seen whether cbPMP31 or cbPMP32 can compensate for the loss of scPmp27p in Δ*pmp27* cells. The function of cbPMP31p or cbMPM32p is unknown.

Morphologically Distinct Peroxisomal Domains

Not surprisingly, immunoelectron microscopy yielded localization of Pmp27p-HA to the periphery of isolated peroxisomes, consistent with Pmp27p being a membrane protein

(Fig. 11 *A*). However, immunoelectron microscopy of frozen thin sections of oleate induced cells showed not only labeling of the membrane surrounding the dense spherical peroxisomes, but also labeling of closely associated tubular regions (Fig. 11, *B* and *C*). These extensions might correspond to the reported catalase negative loops and tubular extensions of spherical peroxisomes that have been seen before in mammalian cells (Lazarow et al., 1980; Lazarow and Fujiki, 1985; Yamamoto and Fahimi, 1987; Baumgart et al., 1989). Thus, *S. cerevisiae* peroxisomes, as mammalian peroxisomes, appear to consist of morphologically distinct domains. Some of the tubular peroxisomal extensions observed might interconnect bulbous peroxisomes in *S. cerevisiae* (Fig. 11 *D*) to form a peroxisomal reticulum as found in mammalian organisms (Lazarow et al., 1980; Gorgas, 1984; Yamamoto and Fahimi, 1987).

Consistent with the presence of tubular extensions in peroxisomes of *S. cerevisiae* are the finger-like and vesicular extensions that we found to be associated with isolated peroxisomes (Fig. 3). Similar extensions of peroxisomal membranes have been observed in isolated mammalian peroxisomes (Lüers et al., 1993). These structures could be interpreted as buds pinching off mature peroxisomes. However, these structures could also be remnants of tubular extensions of peroxisomes or tubular connections between peroxisomes that remain attached to the peroxisomes during homogenizatin and cell fractionation. More distal regions of the tubular peroxisomal domains might be fragmented into small, light vesicles. Our data also suggest that peroxisomes of increased density arise from lighter preforms during induction (Fig. 2). One interpretation of this results could be that the observed light membranes represent small spherical organelles that increase in density during induction as a consequence of massive protein import and enlargement. However, if the light fraction would represent tubular membranes, much of the inconspicuous peroxisomal compartment in noninduced *S. cerevisiae* may consist of tubular peroxisomal domains rather than bulbous peroxisomes. During oleic acid induction in *S. cerevisiae*, bulbous peroxisomes might arise by local dilations of tubular peroxisomal segments.

Besides the finger-like extensions, the isolated peroxisomes also showed the presence of a dense submembranous layer that was absent in the finger-like extension (Fig. 3 *A*). This dense layer may prevent tight resealing of the surrounding peroxisomal membrane after injury during homogenization and cell fractionation, particularly if this layer is rigid and not readily deformable. The membrane leakiness that is ascribed to isolated peroxisomes could be caused by ruptured and incompletely resealed membranes overlying this cortical layer. Poxlp is among the major constituents of this cortical layer. It remains to be seen whether this layer represents a physiologically relevant interaction of the matrix with the overlying membrane.

Function of Pmp27p

Deletion of the PMP27 gene yielded cells with normal growth on glucose or ethanol, but with impaired growth on oleate. When grown under noninducing conditions, wild-type and Δ*pmp27* mutant cells did not differ with respect to size and number of peroxisomes (Fig. 12 *B*), suggesting that Pmp27p is not required for the division and inheritance of
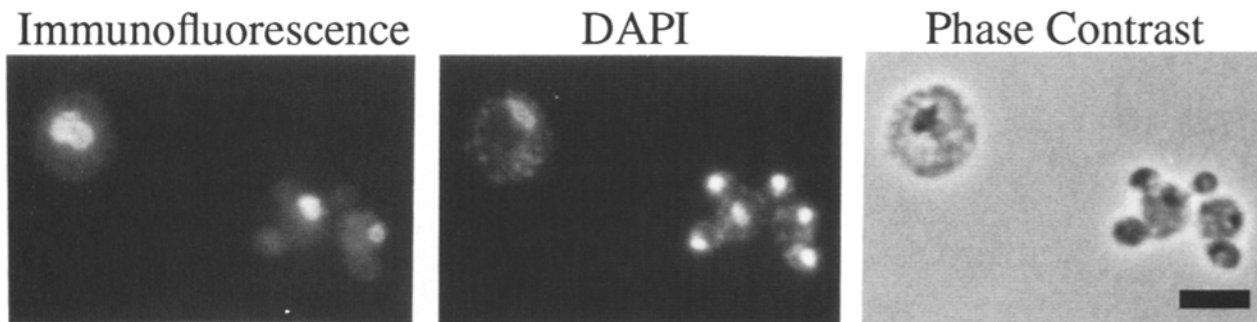
Immunofluorescence   DAPI   Phase Contrast

Figure 15. Immunofluorescence microscopy localization of thiolase in multibudded Δ*pmp27* mutant cells. Cells were induced for 48 h on oleic acid medium. The panels show either thiolase localization by immunofluorescence, DAPI staining of DNA by fluorescence, or phase contrast micrographs of the same cells. The mutant phenotype was characterized by the presence of giant peroxisomes in mother cells but absence of peroxisomes in cell buds. Nuclei were present in both, mother cells and buds. Thiolase localization was determined using a polyclonal antiserum against the enzyme and FITC-labeled donkey anti–rabbit antiserum. Bar, 10 μm.

peroxisomes under noninducing conditions. During oleic acid induction, however, a progressive decrease in the number of peroxisomes per mutant cell was observed, and at later stages of induction, the few mutant peroxisomes were considerably larger than those in induced wild-type cells (Figs. 12 and 13). Failure of the Δ*pmp27* cells in parceling mature peroxisomes into smaller quanta may be the reason for their overproportional enlargement during induction. The Δ*pmp27* mutant phenotype is also characterized by the formation of multiple buds upon growth in oleic acid medium (Fig. 14). This result does not only indicate that the mother cells survived on oleic acid medium, but it also suggests that the cells metabolize oleic acid, which requires functional peroxisomes. Thus the giant peroxisomes observed might still fulfill their function in oleic acid metabolism. This is also in agreement with the comparison of the protein composition of purified wild-type and mutant peroxisomes which, except for the absence of Pmp27p, did not reveal significant differences (data not shown). As the majority of the cell buds of oleic acid–induced Δ*Pmp27* mutant cells do not contain peroxisomes (Fig. 15), the inability of the mutant cells to grow on oleic acid is more likely caused by a defect in peroxisomal inheritance. However, as distribution of peroxisomes to daughter cells in Δ*pmp27* mutant cells still occurs to some extent at early time points of induction (data not shown), Pmp27p does not seem to be directly involved in migration of peroxisomes during mitosis. One simple explanation for the inheritance defect could be that the peroxisomes in Δ*pmp27* mutant cells may be too large to pass into the bud. However, even if the giant peroxisomes could become inherited, because of the suggested defect in parceling of mature peroxisomes, there would be no peroxisomes left to inherit after a few generations. Recently two yeast mutants with a defect in mitochondrial inheritance have been described (Sogo and Yaffe, 1994; Burgess et al., 1994). These mutants are characterized by the presence of giant mitochondria that cannot be inherited to the daughter cells. In both cases, this phenotype is caused by defects in mitochondrial outer membrane proteins. It was suggested that mitochondrial morphology is maintained by binding of these proteins to the cytoskeleton. Likewise, if in *S. cerevisiae* the structure of peroxisomes or of a peroxisomal reticulum is maintained by the cytoskeleton, Pmp27p may serve as a peroxisomal membrane anchor to the cytoskeleton. The identification of

proteins that interact with Pmp27p will provide further insight into molecular mechanisms regulating the morphology, proliferation, and inheritance of peroxisomes.

References

Aitchison, J. D., W. W. Murray, and R. A. Rachubinski. 1991. The carboxy-terminal tripeptide Ala-Lys-Ile is essential for targeting *Candida tropicalis* trifunctional enzyme to yeast peroxisomes. *J. Biol. Chem.* 266:23197–23303.

Avers, C. J., and M. Federman. 1968. The occurence in yeast of cytoplasmic granules which resemble microbodies. *J. Cell. Biol.* 37:555–559.

Ausubel, F. M., R. Brent, R. E. Kingston, D. D. Moore, J. G. Seidman, J. A. Smith, and K. Struhl. 1992. Short Protocols in Molecular Biology. Green Publishing Associates, New York.

Baumgart, E., A. Völkl, T. Hashimoto, and H. D. Fahimi. 1989. Biogenesis of peroxisomes: immunocytochemical investigation of peroxisomal membrane proteins in proliferating rat liver peroxisomes and in catalase-negative membrane loops. *J. Cell. Biol.* 108:2221–2231.

Bradford, M. M. 1976. A rapid and sensitive method for the quantification of microgram quantities of protein utilizing the principle of protein-dye binding. *Anal. Biochem.* 72:248–254.

Bruschi, C. V., A. R. Comer, and G. A. Howe. 1987. Specificity of DNA uptake during whole cell transformation of *S. cerevisiae. Yeast.* 3:131–137.

Burgess, S. M., M. Delannoy, and R. E. Jensen. 1994. MMM1 encodes a mitochondrial outer membrane protein essential for establishing and maintaining the structure of yeast mitochondria. *J. Cell Biol.* 126:1375–1391.

Dijken van, J. P., M. Veenhuis, C. A. Vermeulen, and W. Harder. 1975. Cytochemical localization of catalase activity in methanol- grown Hansenula polymorpha. *Arch. Microbiol.* 105:261–267.

Dmochowska, A., D. Dignard, R. Maleszka, and D. Y. Thomas. 1990. Structure and transcriptional control of the *Saccharomyces cerevisiae POX1* gene encoding acryl coenzyme A oxidase. *Gene (Amst.).* 88:247–252.

Douma, A. C., M. Veenhuis, W. de Koning, and W. Harder. 1985. Dihydroxyacetone synthase is localized in the peroxisomal matrix of methanol grown Hansenula polymorpha. *Arch. Microbiol.* 143:237–243.

Einerhand, A. W. C., W. T. Kos, B. Distel, and H. F. Tabak. 1993. Characterization of a transcriptional control element involved in proliferation of peroxisomes in yeast in respone to oleate. *Eur. J. Biochem.* 214:323–331.

Erdmann, R., M. Veenhuis, D. Mertens, and W. H. Kunau. 1989. Isolation of peroxisome-deficient mutants of *Saccharomyces cerevisiae. Proc. Natl. Acad. Sci. USA.* 86:5419–5423.

Erdmann, R., F. F. Wiebel, A. Flessau, J. Rytka, A. Beyer, K. U. Fröhlich, and W. H. Kunau. 1991. *PAS1*, a yeast gene required for peroxisome biogenesis, encodes a member of a novel family of putative ATPases. *Cell.* 64:499–510.

Erdmann, R., and W. H. Kunau. 1994. Purification and immunolocalization of

3-oxoacyl-CoA thiolase from *Saccharomyces cerevisiae*. *Yeast*. 10:1173–1182.

Erdmann, R. 1994. The peroxisomal targeting signal of 3-oxoacyl-CoA thiolase from *Saccharomyces cerevisiae*. *Yeast*. 10:935–944.

Farguhar, M. G., and G. E. Palade. 1965. Cell junctions in amphibian skin. *J. Cell. Biol.* 26:263–291.

Field, J., J. Nikawa, D. Broek, B. MacDonald, L. Rodgers, I. A. Wilson, R. A. Lerner, and M. Wigler. 1988. Purification of a RAS- responsive adenylyl cyclase complex from *Saccharomyces cerevisiae* by use of an epitope addition method. *Mol. Cell. Biol.* 8:2159–2165.

Fukui, S., S. Kawamoto, S. Yasuhara, and A. Tanaka. 1975. Microbody of methanol-grown yeasts. *Eur. J. Biochem.* 59:561–566.

Fujiki, Y., S. Fowler, H. Shio, A. L. Hubbard, and P. B. Lazarow. 1982. Polypeptide and phsopholipid composition of rat liver peroxisomes: comparison with endoplasmic reticulum and mitochondrial membranes. *J. Cell. Biol.* 93:103–110.

Gorgas, K. 1984. Peroxisomes in sebaceous glands. V. Complex peroxisomes in the mouse preputial gland: serial sectioning and three-dimensional reconstruction studies. *Anat. Embryol.* 169:261–270.

Gould, S. J., G. A. Keller, N. Hosken, J. Wilkinson, and S. Subramani. 1989. A conserved tripeptide sorts proteins to peroxisomes. *J. Cell Biol.* 108:1657–1664.

Gould, S. J., D. McCollum, A. P. Spong, J. A. Heyman, and S. Subramani. 1992. Development of the yeast Pichia pastoris as a model organism for a genetic and molecular analysis of peroxisome assembly. *Yeast*. 8:613–628.

Griffiths, G. K., C. Simmons, K. Warren, and K. T. Tokuyasu. 1983. Immunoelectron microscopy using thin frozen sections: applications to studies of the intracellular transport of Semliki forest virus spike glycoproteins. *Methods Enzymol.* 96:466–485.

Höhfeld, J., M. Veenhuis, and W. H. Kunau. 1991. *PAS3*, a *Saccharomyces cerevisiae* gene encoding a peroxisomal integral membrane protein essential for peroxisome biogenesis. *J. Cell Biol.* 114:1167–1178.

Jones, J. S., and L. Prakash. 1990. Yeast *Saccharomyces cerevisiae* selectable markers in pUC18 polylinkers. *Yeast*. 6:363–366.

Kaldi, K., P. Diestelkötter, G. Stenbeck, S. Auerbach, U. Jäckle, H. J. Mägert, F. T. Wieland, and W. W. Just. 1993. Membrane topology of the 22 kDa integral membrane protein. *FEBS (Fed. Eur. Biochem. Soc.) Lett.* 315:217–222.

Kamijo, K., S. Taketani, S. Yokota, T. Osumi, and T. Hashimoto. 1990. The 70-kDa peroxisomal membrane protein is a member of the Mdr (P-glycoprotein)-related ATP-binding superfamily. *J. Biol. Chem.* 265:4534–4540.

Kamijo, K., T. Kamijo, I. Ueno, T. Osumi, and T. Hashimoto. 1992. Nucleotide sequence of the human 70 kDa peroxisomal membrane protein. *Biochim. Biophys. Acta*. 1129:323–327.

Kamiryo, T., M. Abe, K. Okazaki, S. Kato, and N. Shimamoto (1982). Absence of DNA in peroxisomes from *Candida tropicalis*. *J. Bacteriol.* 152:269–274.

Kyte, J., and R. F. Doolittle. 1982. A simple method for displaying the hydropathic character of a protein. *J. Mol. Biol.* 157:105–132.

Lazarow, P. B., H. Shio, and M. Robbi. 1980. Biogenesis of peroxisomes and the peroxisome reticulum hypothesis. *In* Biological Chemistry of Organelle Formation. T. Bucher, W. Sebald, H. Weiss, editors. Springer-Verlag, New York. pp. 187–206.

Lazarow, P. B., and Y. Fujiki. 1985. Biogenesis of peroxisomes. *Annu. Rev. Cell. Biol.* 1:489–530.

Lazarow, P. B. 1988. Peroxisomes. *In* The Liver: Biology and Pathology. J. M. Arias, W. B. Jakoby, H. Popper, D. Schlachter, and D. A. Shafritz, editors. Raven Press Ltd., New York. pp. 241–254.

Lüers, G., T. Hashimoto, H. D. Fahimi, and A. Völkl. 1993. Biogenesis of peroxisomes: isolation and characterization of two distinct peroxisomal populations from normal and regenerating rat liver. *J. Cell. Biol.* 121:1271–1280.

McCammon, M. T., C. A. Dowds, K. Orth, C. R. Moomaw, C. A. Slaughter, and J. M. Goodman. 1990*a*. Sorting of peroxisomal membrane protein PMP47 from *Candida biodinii* into peroxisomal membranes of *Saccharomyces cerevisiae*. *J. Biol. Chem.* 265:20098–20105.

McCammon, M. T., M. Veenhuis, S. B. Trapp, and J. M. Goodman. 1990*b*. Association of glyoxylate and beta-oxidation enzymes with peroxisomes of *Saccharomyces cerevisiae*. *J. Bacteriol.* 172:5861–5827.

Moreno, M., R. Lark, K. L. Campbell, and J. M. Goodman. 1994. The peroxisomal membrane proteins of *Candida boidinii*: gene isolation and expression. *Yeast*. 10:1447–1457.

Moreno de la Garza, M., U. Schultz-Borchardt, J. W. Crabb, and W. H. Kunau. 1985. Peroxisomal β-oxidation system of *Candida tropicalis*. *Eur. J. Biochem.* 148:285–291.

Mosser, J., A. M. Douar, C. O. Sarde, P. Kioschis, R. Feil, H. Moser, A. M. Poustka, J. L. Mandel, and P. Aubourg. 1993. Putative X-linked adrenoleukodystrophy gene shares unexpected homology with ABC transporters. *Nature (Lond.)*. 361:726–730.

Osumi, M., N. Miwa, Y. Teranishi, A. Tanaka, and S. Fukui. 1974. Ultrastructure of *Candida* yeasts grown on n-alkanes. *Arch. Microbiol.* 99:181–201.

Pain, D., H. Murakami, and G. Blobel. 1990. Identification of a receptor for protein import into mitochondria. *Nature (Lond.)*. 347:444–449.

Paul, C., and J. P. Rosenbusch. 1985. Folding patterns of porin and bacteriorhodopsin. *EMBO (Eur. Mol. Biol. Organ.) J.* 4:1593–1597.

Reynolds, E. S. 1963. The use of lead citrate at high pH as an electron-opaque stain in electron microscopy. *J. Cell. Biol.* 17:208–213.

Roggenkamp, R., H. Sahm, W. Hinkelmann, and F. Wagner. 1975. Alcohol oxidase and catalase in peroxisomes of methanol-grown *Candida biodinii*. *Eur. J. Biochem.* 59:231–236.

Rose, M. D., P. Novick, J. H. Thomas, D. Bothstein, and G. R. Fink. 1987. A *Saccharomyces cerevisiae* genomic plasmid bank based on a centromere-containing shuttle vector. *Gene (Amst.)*. 60:237–243.

Rose, M. D., L. M. Misra, and J. P. Vogel. 1989. *KAR2*, a karyogamy gene, is the yeast homolog of the mammalian BiP/GRP78 Gene. *Cell*. 57: 1211–1221.

Rothstein, R. 1991. Targeting, disruption, replacement, and allele rescue: integrative DNA transformation in yeast. *Methods Enzymol.* 194:281–301.

Rout, M. P., and J. V. Kilmartin. 1990. Components of the yeast spindle pole body. *J. Cell. Biol.* 111:1913–1927.

Shimosawa, N., T. Tsukamoto, Y. Suzuki, T. Orii, Y. Shirayoshi, T. Mori, and Y. Fujiki. 1992. A human gene responsible for Zellweger syndrome that affects peroxisome assembly. *Science (Wash. DC)*. 255:1132–1134.

Sogo, L. F., and P. Yaffe. 1994. Regulation of mitochondrial morphology and inheritance by Mdm10p, a protein of the mitochondrial outer membrane. *J. Cell Biol.* 126:1361–1373.

Struhl, K. 1987. Promotors, activator proteins, and the mechanism of transcriptional initiation in yeast. *Cell*. 49:295–297.

Subramani, S. 1992. Targeting of proteins into the peroxisomal matrix. *J. Membrane Biol.* 125:88–106.

Swinkels, B. W., S. J. Gould, A. G. Bodnar, R. A. Rachubinski, and S. Subramani. 1991. A novel, cleavable peroxisomal targeting signal at the amino-terminus of the rat 3-ketoacyl-CoA thiolase. *EMBO (Eur. Mol. Biol. Organ.) J.* 10:3255–3262.

Szabo, A. S., and C. J. Avers. 1969. Some aspects of regulation of peroxisomes and mitochondria in yeast. *Ann. NY Acad. Sci.* 168:302–312.

Tokuyasu, K. T. 1973. A technique for ultracryotomy of cell suspension and tissue. *J. Cell. Biol.* 57:551–565.

Towbin, H., T. Staehelin, and J. Gordon. 1979. Electrophoretic transfer of proteins from polyacrylamide gels to nitrocellulose sheets: procedure and some applications. *Proc. Natl. Acad. Sci. USA*. 76:4350–4354.

Tsukamoto, T., S. Miura, and Y. Fujiki. 1991. Restoration by a 35K membrane protein of peroxisome assembly in a peroxisome-deficient mammalian cell mutant. *Nature (Lond.)*. 350:77–81.

Van der Leij, I., M. M. Franse, Y. Elgersma, B. Distel, and H. Tabak. 1993. *PAS10* is a tetratricopeptide-repeat protein that is essential for the import of most matrix proteins into peroxisomes of *Saccharomyces cerevisiae*. *Proc. Natl. Acad. Sci. USA*. 90:11782–11786.

Veenhuis, M., I. Keizer, and W. Harder. 1979. Characterization of peroxisomes in glucose-grown *Hansenula polymorpha* and their development after transfer of cells into methanol containing media. *Arch. Microbiol.* 120:167–175.

Veenhuis, M., M. Mateblowski, W. H. Kunau, and W. Harder. 1987. Proliferation of microbodies in *Saccharomyces cerevisiae*. *Yeast*. 3:77–84.

Veenhuis, M. and J. M. Goodman. 1990. Peroxisomal assembly: membrane proliferation precedes the induction of the abundant matrix proteins in the methylotrophic yeast *Candida boidinii*. *J. Cell Sci.* 96:583–590.

Veenhuis, M., and W. Harder. 1991. Microbodies. *In* The Yeasts. Vol. 4. A. H. Rose and J. S. Harrison, editors. Academic Press, London. pp. 601–653.

Wiebel, F. F., and W. H. Kunau. 1992. The Pas2 protein essential for peroxisome biogenesis is related to ubiquitin-conjugating enzymes. *Nature (Lond.)*. 359:73–76.

Wilson, I. A., H. L. Niman, R. A. Houghten, A. R. Cherenson, M. L. Connolly, and R. A. Lerner. 1984. The structure of an antigenic determinant in a protein. *Cell*. 37:767–778.

Wozniak, R. W., G. Blobel, and M. P. Rout. 1994. POM152 is an integral protein of the pore membrane domain of the yeast nuclear envelope. *J. Cell. Biol.* 125:31–42.

Yaffee, M. P., and G. Schatz. 1984. Two nuclear mutations that block mitochondrial protein import in yeast. *Proc. Natl. Acad. Sci. USA*. 81:4819–4823.

Yamamoto, K., and H. D. Fahimi. 1987. Three-dimensional reconstruction of a peroxisomal reticulum in regenerating rat liver: evidence of interconnections between heterogeneous segments. *J. Cell. Biol.* 105:713–722.

Zaret, K. S., and F. Sherman. 1982. DNA sequence required for efficient transcription termination in yeast. *Cell*. 28:563–573.